Smart Structures and Systems, *Vol. 32, No. 2 (2023) 101-109*
https://doi.org/10.12989/sss.2023.32.2.101

Piezoelectric 6-dimensional accelerometer cross coupling compensation algorithm based on two-stage calibration

Dengzhuo Zhang [a], Min Li [b], Tongbao Zhu [c], Lan Qin [d], Jingcheng Liu [d] and Jun Liu*

The Key Laboratory of Optoelectronic Technology and Systems of Ministry of Education, College of Optoelectronic Engineering, Chongqing University, Chongqing 400044, China

(*Received August 20, 2021, Revised August 16, 2023, Accepted August 16, 2023*)

Abstract. In order to improve the measurement accuracy of the 6-dimensional accelerometer, the cross coupling compensation method of the accelerometer needs to be studied. In this paper, the non-linear error caused by cross coupling of piezoelectric six-dimensional accelerometer is compensated online. The cross coupling filter is obtained by analyzing the cross coupling principle of a piezoelectric six-dimensional accelerometer. Linear and non-linear fitting methods are designed. A two-level calibration hybrid compensation algorithm is proposed. An experimental prototype of a piezoelectric six-dimensional accelerometer is fabricated. Calibration and test experiments of accelerometer were carried out. The measured results show that the average non-linearity of the proposed algorithm is 2.2628% lower than that of the least square method, the solution time is 0.019382 seconds, and the proposed algorithm can realize the real-time measurement in six dimensions while improving the measurement accuracy. The proposed algorithm combines real-time and high precision. The research results provide theoretical and technical support for the calibration method and online compensation technology of the 6-dimensional accelerometer.

Keywords: 6-dimensional accelerometer; compensation algorithm; cross coupling; non-linearity; two-stage calibration

1. Introduction

The 6-dimensional accelerometer can sense the linear acceleration (A_x,A_y,A_z) and angular acceleration (a_x,a_y,a_z) of the object in 3-dimensional space in the Fig. 1. It not only can be gained through the integral operation object in the location of the 3-dimensional space, but also can get space motion of the object, the navigation (Noureldin *et al.* 2009, Meng *et al*. 2019), aerospace field (Santoli *et al*. 2020), the robot control (Li *et al*. 2020), vehicle testing (Peng and Golnaraghi 2004), and other industrial fields, has significant application value.

The 6-dimensional accelerometer in the key is to improve the precision of the engineering application. For the 6-dimensional accelerometer, both calibration data and test results are expected to be in a "linearity" state, while their "non-linearity" state will reduce the real-time measurement accuracy. Cross-coupling is an unavoidable problem of the six-dimensional accelerometer, which will seriously affect the measurement accuracy of the accelerometer. (Zhou *et al*. 2015), which is also one of the main factors for the "non-linearity" state of the accelerometer. Research on calibration and compensation

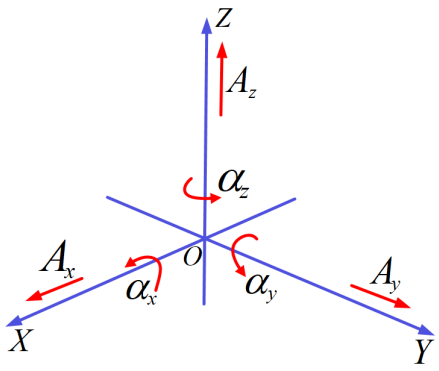

Fig. 1 Schematic diagram of 6-dimensional acceleration

methods based on cross coupling of the six-dimensional accelerometers is essential to improve sensor accuracy (Lin and Sun 2019). The 6-dimensional accelerometer has 2 types: one of which is the integrated 6-dimensional accelerometer about multiple uniaxial accelerometers (IMAA) (Wang and Yuan 2011), and the other one is a 6-dimensional accelerometer for a single mass block-spring-damping system (ASMD). There are bottleneck problems in the IMAA type, such as complicated calibration technology, difficulty in miniaturization, and serious cross-coupling. The ASMD type also has cross-coupling, but it can be further reduced using calibration and arithmetic. Therefore, researches on 6-dimensional accelerometer are mostly focused on ASMD type. No matter what kind of 6-dimensional accelerometer is studied, it is necessary to study the compensation method for the cross coupling of the accelerometer to overcome the cross-coupling and

*Corresponding author, Ph.D., Professor,
E-mail: junliu@cqu.edu.cn
[a] Ph.D. Student
[b] Ph.D., Senior Experimentalist (Professor level)
[c] M.D.
[d] Ph.D., Professor

ISSN: 1738-1584 (Print), 1738-1991 (Online)

improve the accuracy of measurement. There are two standard compensation methods: hardware circuit compensation and software algorithm compensation. However, the hardware circuit compensation is usually expensive, and it is hard to completely and fundamentally eliminate the effects brought by non-linearity (Sun *et al.* 2016). Compared with the hardware circuit compensation method, the software algorithm compensation is convenient, accurate, and flexible (Wang 2008), but the relevant research results of the 6-dimensional accelerometer are few. Chapsky *et al.* (2007) proposed a segmented PSD 6-dimensional accelerometer and realized the detection of 6-dimensional acceleration information through linear calibration. Zhang *et al*. (2021) established a cross-coupling model based on the six-dimensional accelerometer, and verified the correctness of the model by calibration technology. The above results further improve the calibration technology of the 6-dimensional accelerometer but do not compensate for the non-linear error caused by cross coupling. The 6-dimensional force sensor and the 6-dimensional accelerometer belong to the same category of multi-dimensional sensors. Wang *et al*. (2011) used the jacobian matrix to replace the initial state matrix for error compensation about the 6-dimensional force sensor of the Stewart platform, and the algorithm's validity was proved by numerical simulation. Because of the interaction between multiple channels of the 6-dimensional accelerometer, the traditional neural network algorithm is difficult to be applied to the multi-dimensional solution of the 6-dimensional accelerometer. At present, the least square method is mainly used in the research. Zhao *et al*. (2016) used the least square method (LSM) to decouple the 6-dimensional force sensor for the flexible joint 6-UPUR with a large range, and the calibration error was 2.67%. Al-Mai *et al*. (2018) estimated the linear part based on the standard least square method (LSM) linear model for optical fiber six-dimensional force sensors, which reduced the MEAN square error to 0.53%. The above research mainly design for a 6-axis force sensor by the LSM of decoupling method, but there is no sensor cross coupling of non-linear error compensation. Currently, researchers improve the performance of sensors through algorithms. For example, Amini *et al*. (2020) optimize the patch position of sensors through improved genetic algorithms. In order to ensure that the decoding speed at the same time, adequate compensation of cross coupling effect to non-linear error, improve sensor measurement accuracy, we need to research online compensation algorithm based on cross coupling.

Therefore, to compensate for the 6-dimensional accelerometer of cross coupling effect to non-linear error, improve the sensor measurement accuracy, and overcome the contradiction between precision and processing speed, this paper analyzed the piezoelectric 6-dimensional accelerometer principle of cross coupling based on the piezoelectric 6-dimensional accelerometer. Moreover, the online compensation algorithm is put forward given the cross coupling, the piezoelectric 6-dimensional accelerometer prototype is manufactured, and the calibration and tests are performed. The accuracy of the proposed algorithm is tested through calibration and testing. The algorithm compensates for the non-linear error caused by cross coupling and updates the calibration matrix of the accelerometer in real-time to realize online compensation, which has the advantages of fast speed, high precision, and easy transplantation. The research results provide theoretical and technical support for the calibration method and online compensation technology of the 6-dimensional accelerometer.

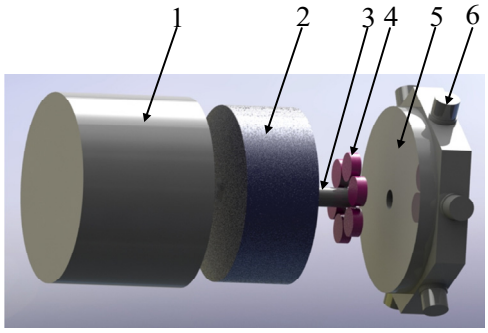

(a) simple diagram of a six-dimensional accelerometer

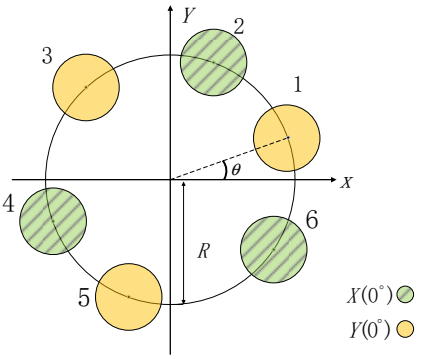

(b) Mechanical analysis of quartz wafer units

Fig. 2 A simplified model of the 6-dimensional accelerometer

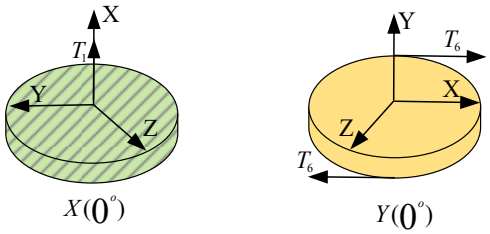

Fig. 3 Loading direction of quartz wafer

2. Cross coupling Compensation algorithm based on Two-level Calibration (CCTC)

The structure diagram of the 6-dimensional accelerometer in this study is shown in Fig. 2(a). Its composition includes the shell (1), mass block (2), preloaded-bolt (3), six piezoelectric quartz wafers (4), base (5), electrode (6), sealing packing, and other compositions.

F_j, M_j ($j = x, y, z$) is the inertial force generated by A_j, a_j ($j=x, y, z$) measured for the accelerometer. f_j, m_j ($j = x, y, z$) is the inertial force component in the sensitive direction of the quartz wafer unit. According to Fig. 3, it can be seen

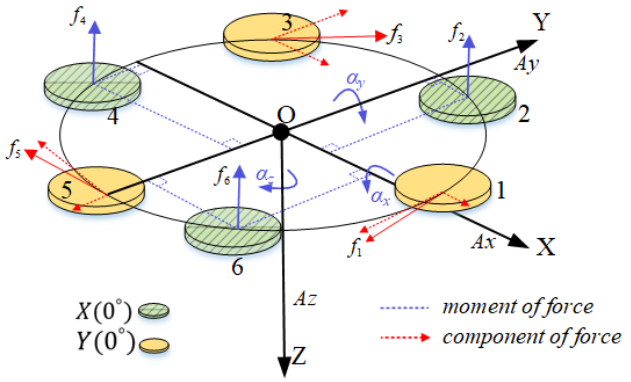

Fig. 4 3D view of the wafer distribution

that the $X(0^{o})$ tangent chip measures the normal force, and $Y(0^{o})$ measures the shear force. The relation between the charge Q_{Fj} $(j = x, y, z)$, Q_{Mj} $(j = x, y, z)$ measured by the accelerometer, and the charge Q_i $(i = 1, 2,\ldots, 6)$ generated by the six wafers is shown in the formula (1).

$$\begin{cases} Q_{F_x} = Q_1 + Q_3 + Q_5 \propto \frac{3}{6} f_x \\ Q_{F_y} = Q_1 + Q_3 + Q_5 \propto \frac{3}{6} f_y \\ Q_{F_z} = Q_2 + Q_4 + Q_6 \propto \frac{3}{6} f_z \\ Q_{M_x} = Q_2 + Q_4 + Q_6 \propto \frac{3}{6} m_x \\ Q_{M_y} = Q_2 + Q_4 + Q_6 \propto \frac{3}{6} m_y \\ Q_{M_z} = Q_1 + Q_3 + Q_5 \propto \frac{3}{6} m_z \end{cases} \tag{1}$$

According to the mechanical analysis of the quartz wafer unit in Fig. 4, the compound conversion formula between the six directions inertia force of the accelerometer and the quartz wafer can be obtained. Then the formula (1) can be converted into formula (2).

$$\begin{cases} Q_{Ax} = Q_1 \sin\theta + Q_3 \sin(\frac{\pi}{3} - \theta) + Q_5 \cos(\theta - \frac{\pi}{6}) \\ Q_{Ay} = Q_1 \cos\theta + Q_3 \cos(\frac{\pi}{3} - \theta) + Q_5 \sin(\theta - \frac{\pi}{6}) \\ Q_{Az} = Q_2 + Q_4 + Q_6 \\ Q_{\alpha x} = Q_2 \cos(\theta - \frac{\pi}{6}) - Q_4 \sin\theta - Q_6 \sin(\frac{\pi}{3} - \theta) \\ Q_{\alpha y} = Q_2 \cos(\theta - \frac{\pi}{6}) - Q_4 \sin\theta - Q_6 \sin(\frac{\pi}{3} - \theta) \\ Q_{\alpha z} = Q_1 + Q_5 - Q_3 \end{cases} \tag{2}$$

The $Q_1, Q_2, \ldots, Q_6$ represent the charge of 6 quartz wafer units, and the $Q_{A_x}, Q_{A_y}, \ldots, Q_{\alpha_z}$ represent the charge of 6 directions.

Let the coefficient matrix T of $Q_i(i = 1, 2,\ldots, 6)$ be

$$T = \begin{bmatrix} \sin\theta & 0 & \sin(\frac{\pi}{3} - \theta) & 0 & \cos(\theta - \frac{\pi}{6}) & 0 \\ \cos\theta & 0 & \cos(\frac{\pi}{3} - \theta) & 0 & \sin(\theta - \frac{\pi}{6}) & 0 \\ 0 & 1 & 0 & 1 & 0 & 1 \\ 0 & \cos(\theta - \frac{\pi}{6}) & 0 & \sin\theta & 0 & \sin(\frac{\pi}{3} - \theta) \\ 0 & \sin(\theta - \frac{\pi}{6}) & 0 & \cos\theta & 0 & \cos(\frac{\pi}{3} - \theta) \\ 1 & 0 & 1 & 0 & 1 & 0 \end{bmatrix} \tag{3}$$

Let T be a cross coupling filter, then the input-output relationship of the sensor is

$$\mathrm{Y} = \begin{bmatrix} A_x \\ A_y \\ A_z \\ \alpha_x \\ \alpha_y \\ \alpha_z \end{bmatrix} = T * \begin{bmatrix} Q_1 \\ Q_2 \\ Q_3 \\ Q_4 \\ Q_5 \\ Q_6 \end{bmatrix} * G \tag{4}$$

The loaded 6-dimensional acceleration is denoted as Lo_{ij}, the $i = A_x, A_y, A_z, \alpha_x, \alpha_y, \alpha_z$, $j = 1,2, \ldots, m$. The m is the loads times, and the response output of the accelerometer about each direction is Q_{ij}. The inverse matrices C_i and C_i' of the matrix G are obtained through linear fitting by the least square and polynomial fitting method, as shown in Formula (5).

$$\begin{cases} C_i = \frac{n(\sum i_j Q_{ij}) - (\sum i_j)(\sum Q_{ij})}{n(\sum {i_j}^2) - (\sum i_j)^2} \\ C_i' = \frac{k_0 + k_1 Q_{ij} + k_2 {Q_{ij}}^2 + \cdots + k_n {Q_{ij}}^n}{Q_{ij}} \\ \sum_{j=1}^{n} \left(\sum_{t=0}^{n} k_t {Q_{ij}}^t - Lo_{ij} \right)^2 = Min \end{cases} \tag{5}$$

In Formula (4), $i = A_x, A_y, A_z, \alpha_x, \alpha_y, \alpha_z$, $j = 1, 2, \ldots, m$. The m is the loads times, and the linearity of the accelerometer determines the value of n. The k_n and the k_t are coefficients of the polynomial fitting. Then the solution formula of the 6-dimensional accelerometer is as follows

$$Y = T * \begin{bmatrix} Q_1 \\ Q_2 \\ Q_3 \\ Q_4 \\ Q_5 \\ Q_6 \end{bmatrix}_t C^{-1} = T * \begin{bmatrix} Q_1 \\ Q_2 \\ Q_3 \\ Q_4 \\ Q_5 \\ Q_6 \end{bmatrix}_{t-1} * (C^{-1} + kC'^{-1} - kC^{-1}) \tag{6}$$

Where t represents the time t, let $kTQC'^{-1}$ be the non-linear solution output k times, and $kTQC^{-1}$ be the linear solution output k times, both of which obey the Gaussian distribution, then $k^2TQC'^{-1}C^{-1}$ also obey the Gaussian distribution, then K value in Eq. (6) is Eq. (7).

$$K = \frac{\sigma_1^2 \sigma_2^2}{\sigma_1^2 + \sigma_2^2} \tag{7}$$

Where σ_1 and σ_2 are the variances of two Gaussian distributions, respectively, the K value is the update factor used to adjust the proportion of mixed output adaptively.

The algorithm flow chart is shown in Fig. 5.

$$C = \begin{bmatrix} 1.0312 & 0.6150 & 2.7288 & -2.9042 & -3.8070 & 1.6806 \\ -3.9313 & 3.3444 & 3.0523 & -1.0322 & 1.2580 & -2.2789 \\ 0.2188 & -1.6303 & -0.3704 & -1.1184 & 0.1833 & -1.1297 \\ 0.0039 & -0.0049 & -0.0031 & 0.0016 & -0.0012 & 0.0035 \\ 0.0016 & 0.0006 & 0.0022 & -0.0039 & -0.0037 & 0.0029 \\ -0.0039 & -0.0001 & -0.0036 & -0.0001 & -0.0035 & 0.0001 \end{bmatrix} \tag{8}$$

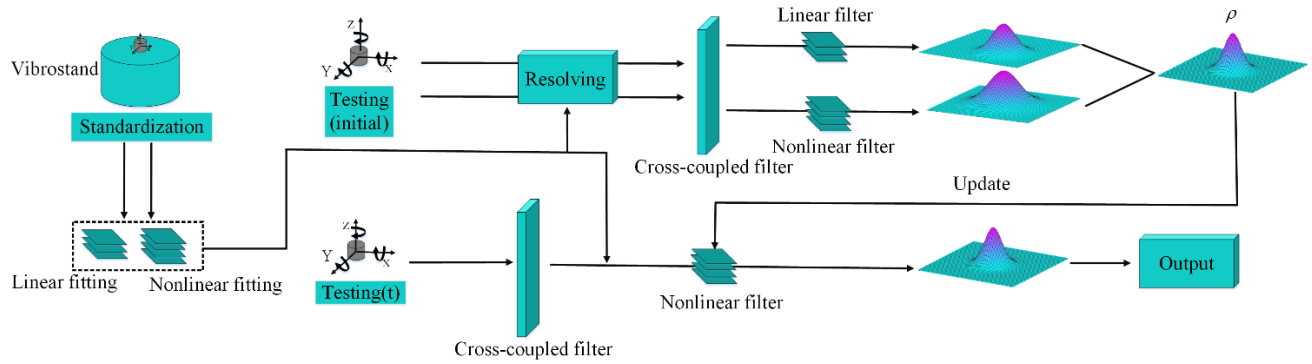

Fig. 5 Algorithm CCTC flow chart

Algorithm **CCTC**

(a) Standardization

1. The linear calibration matrix C_i is obtained through Equation (5).
2. The non-linear calibration matrix $C_i'$is obtained through Equation (5).

(b) Resolving

Input: $Q_1, Q_2, Q_3, Q_4, Q_5, Q_6$

1. Initialize the operation and set the step size coefficient.
2. Cross coupled filter is performed.
3. The corresponding Gaussian distribution is obtained through C_i and C_i'.
4. Calculate the variance σ in two Gaussian distribution
5. K value can be obtained in real-time through Equation (7).
6. Equation (6) is used for iterative calculation, and cross coupled filtering operation is carried out simultaneously.

Output: $A_{xt}, A_{yt}, A_{zt}, a_{xt}, a_{yt}, a_{zt}$

3. Experiment

This work mainly carries out calibration experiments and test experiments, through which the algorithm's validity is verified. The experimental prototype of the piezoelectric 6-dimensional accelerometer is shown in Fig. 7(c).

3.1 Calibration

The calibration method adopts the linear vibrostand and angular vibrostand with a mounting fixture to realize the 6-dimensional acceleration loading. The calibration system is shown in Fig. 7. As the excitation source, the linear vibrostand and angular vibrostand are shown in Fig. 7(a) and (b), respectively. The mounting method of the fixture is shown in Figs. 7(h), (i), (j). In the calibration, the loads range of linear acceleration and angular acceleration is 9.8 m/s^2-362.6 m/s^2, 17.64 rad/s^2-335.12 rad/s^2, with 10 loading points respectively. Moreover, the frequency is set at 160 Hz. The vibrostand produces a sinusoidal signal, and we choose the amplitude of the output sinusoidal signal.

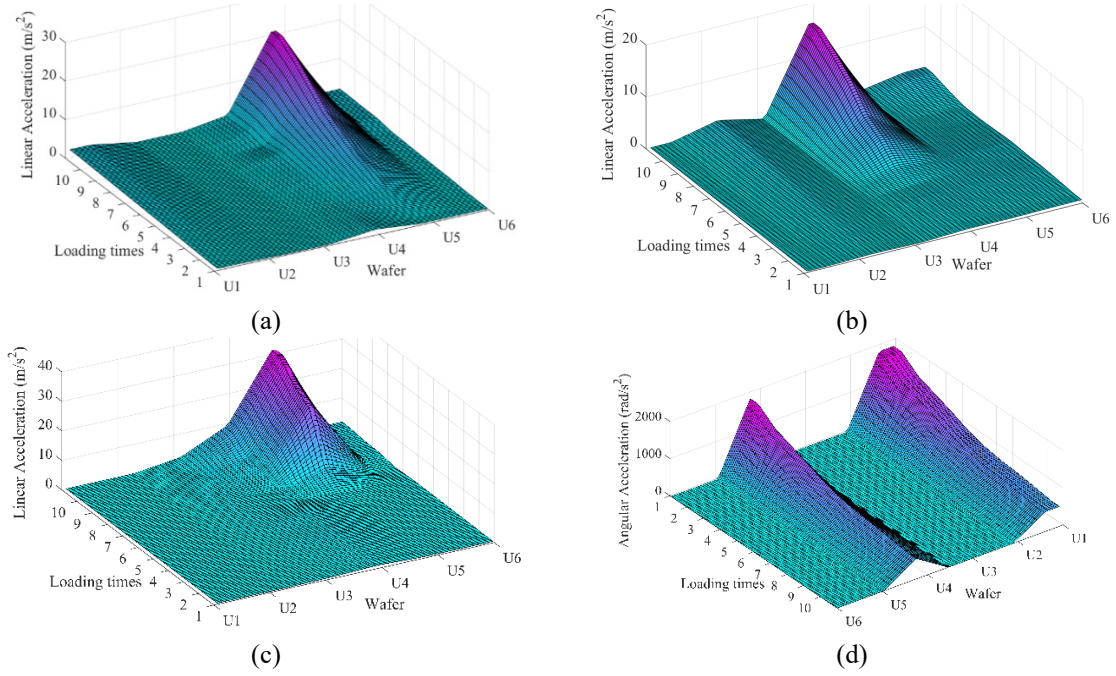

Fig. 6 Least square linear fitting curve

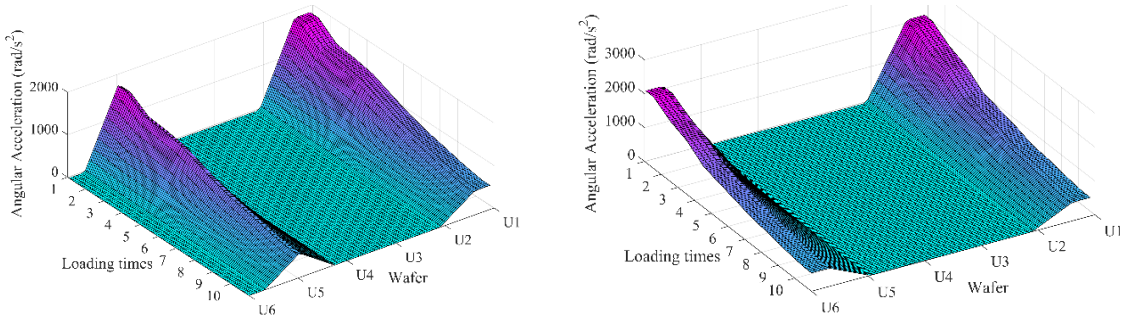

Fig. 6 Continued

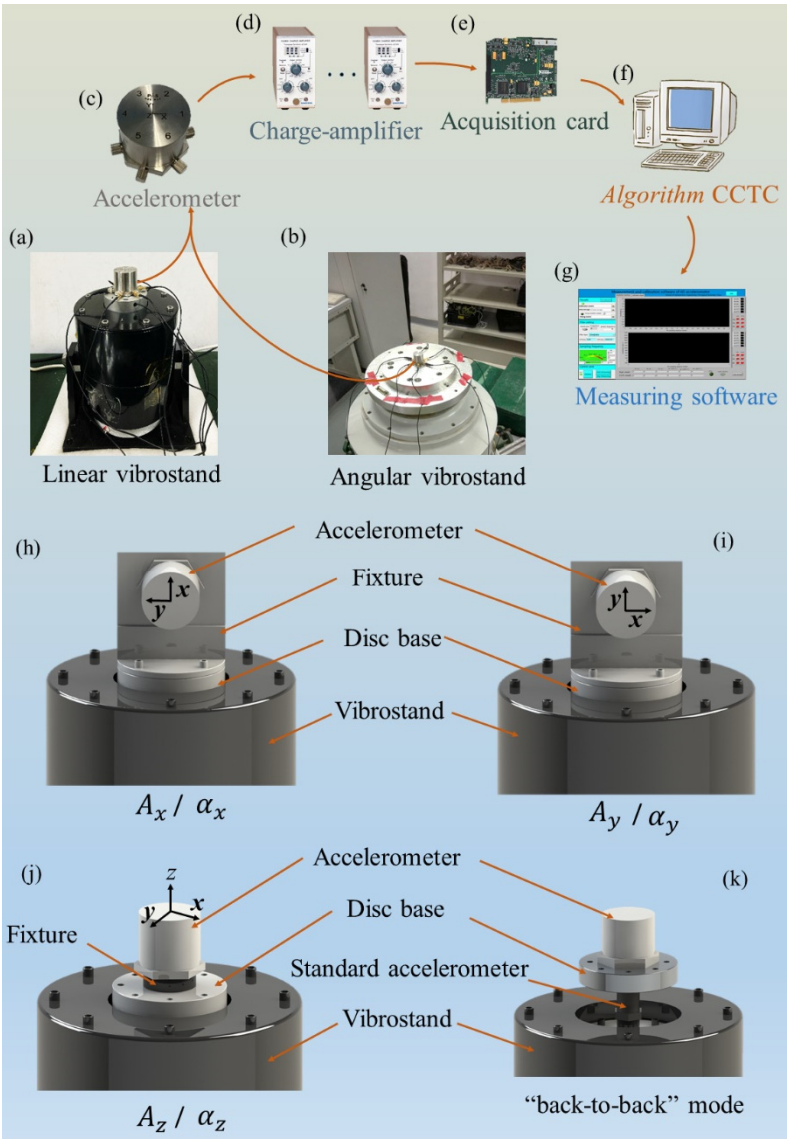

Fig. 7 Experimental platform construction

The calibration method refers to the "back-to-back" mode in IOS 16063-21:2003(E). The installation location is shown in Fig. 7(k). The standard accelerometer is B&K (CA-YD-122 47336). The angular vibrostand uses the output of the vibrostand as the standard.

3.1.1 Linear calibration

The least-square linear fitting curve of the accelerometer's output and input accelerations was obtained by fitting with the least square method, as shown in Fig. 6. In the Fig. 6, the (a), (b), (c), (d), (e), (f) are direction A_x, A_y, A_z, a_x, a_y and a_z, respectively. The linear calibration matrix

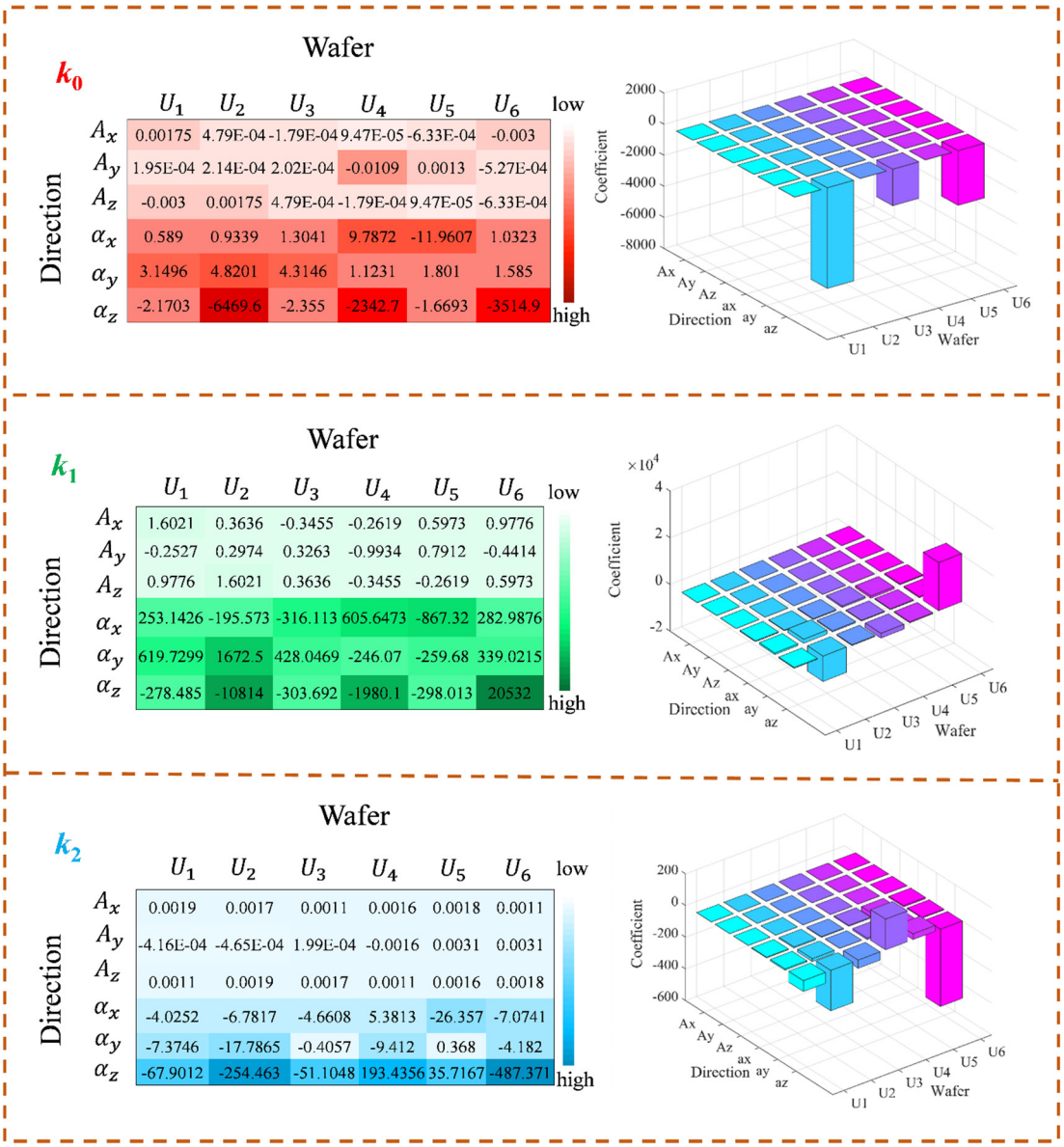

Fig. 8 Polynomial non-linear fitting coefficients

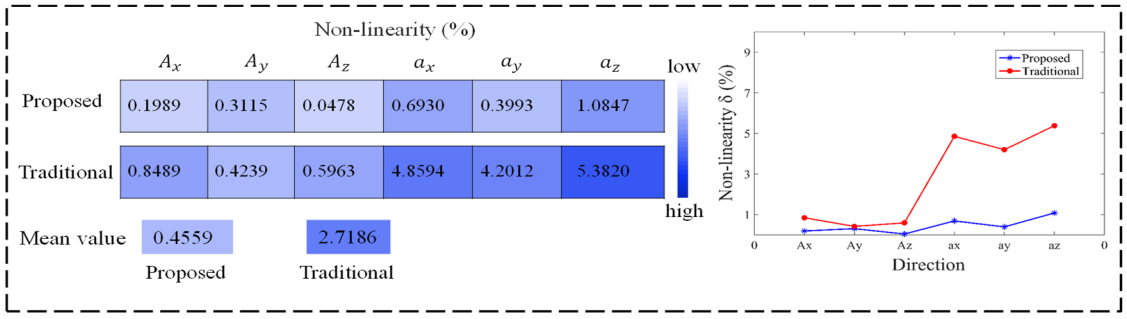

Fig. 9 Comparison of non-linearity δ

C was obtained as shown in Eq. (8).

3.1.2 Non-linear calibration

Based on the actual linearity of the piezoelectric 6-dimensional accelerometer in this word, the n in Eq. (5) is 2, then C_i' is expressed as

$$\begin{cases} C_i' = \dfrac{k_0 + k_1 Q_{ij} + k_2 {Q_{ij}}^2}{Q_{ij}} \\ i = A_x, A_y, A_z, \alpha_x, \alpha_y, \alpha_z \end{cases} \tag{9}$$

Through non-linear fitting of Eq. (5), the values of$k_0, k_1$and k_2 in 6 directions $A_x, A_y, A_z, \alpha_x, \alpha_y, \alpha_z$ are

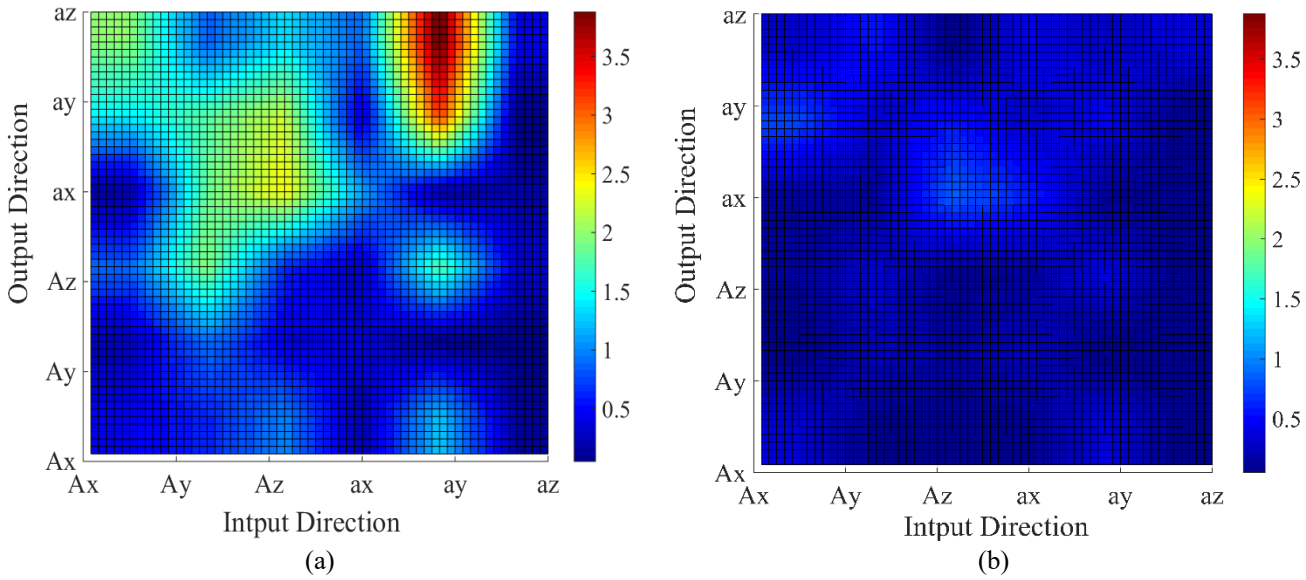

Fig. 11 Temperature chart of average reference error

obtained, as shown in Fig. 8. As shown in Fig. 8, the non-linear fitting coefficient in the angle direction is much larger than that in the line direction.

3.2 Test

In the test experiment, the vibrostand with the mounting fixture is used to realize the single loading of 6-dimensional acceleration, and 10 points are tested in each direction, respectively. The frequency is set at 160 Hz. The output results of the proposed algorithm's test response in six directions are shown in Fig. 10(b). The work is achieved by designing the LabVIEW program, and the calibration and measurement software is shown in Fig. 10(a). As Fig. 10(b) shows, when unidirectional loads are applied to the six directions respectively, the accelerometer can measure the acceleration values in the six directions, and the output of the main direction shows a linear relationship. Let the non-linearity of the main direction δ in the test be expressed as Eq. (10).

$$\delta = \frac{\Delta\gamma\max}{\gamma} * 100\% \tag{10}$$

Where $\Delta\gamma\max$ is the maximum deviation between the curve tested by the sensor and the fitting line, γ is the full-scale output, and the non-linearity δ of the six directions between the proposed method and the traditional method is shown in Fig. 9.

It can be seen from Fig. 9 that the non-linearity of the proposed algorithm in six directions is better than that of the traditional method, and the average non-linearity decreases by 2.2628%.

In this work, the validity of the proposed algorithm is demonstrated by comparing the reference error between the least square fitting method and the proposed algorithm. The two algorithms test 10 points for each direction, respectively, so the average quotation error *Quo* is as shown in Eq. (11).

$$Quo = \frac{1}{m}\sum_{j=1}^{m}\left(\frac{\hat{Y}_j - Y_j}{\gamma}\right) \tag{11}$$

Where $\hat{Y}_j$ is the true value, Y_j is the predicted value, and γ is the full-scale value.

Due to the limitations of experimental equipment, the total range value of the accelerometer cannot be loaded. In this paper, the maximum excitation value loaded in each dimension is selected to replace the total range value of the accelerometer for calculation. A_x, A_y, and A_z take 2 m/s^2 as the total range value, and α_x, α_y, and α_z take 2200 rad/s^2 as the total range value. The Temperature chart of the average reference error of 10 times of loading of the two algorithms is shown in Fig. 11. In the Fig. 11, the (a) is the temperature chart of least square, and the (b) is proposed algorithm. This paper compares the algorithms by calculating the Average Reference Error 2-Norm (ARE-2N) of 6 dimensions.

$$\begin{cases} \mathrm{ARE-2N}_i = \left\| \frac{1}{m}\sum_{j=1}^{m}\left(\frac{\hat{Y}_{ji} - Y_{ji}}{\gamma_i}\right) \right\|_2 \\ \mathrm{i} = A_x, A_y, A_z, \alpha_x, \alpha_y, \alpha_z \end{cases} \tag{12}$$

It can be seen from Fig. 11 that the reference error of the proposed algorithm in six directions is less than that of the least square method in the case of one-dimensional loading in six directions. The total ARE-2N value of the six directions of the proposed algorithm is 4.6309%, and the total ARE-2N value of the six directions of the least square method is 18.4291%. The total ARE-2N value of the six directions of the proposed algorithm is reduced by 13.7982%. This algorithm can effectively reduce the cross coupling error and improve the measurement accuracy.

The uncertainty analysis of the accelerometer is carried out in this paper. Fig. 10(c) shows the uncertainty report. The calculation formula for the uncertainty of class *A* is shown in Eq. (13).

$$u_x = \sqrt{\frac{\sum_{i=1}^{n}(x-\bar{x})^2}{n-1}} \Big/ \sqrt{n-1} \tag{13}$$

In Eq. (13), x is the measured value, $\bar{x}$ is the average value of the measurement, and n is the number of measurements.

The degree of freedom v=n-1. According to the *T*-distribution, the coverage factor k is 2.26. The calculation formula for the expanded uncertainty of measurement U is shown in Eq. (14).

$$U = k * u_x \tag{14}$$

While improving the accuracy of the accelerometer, it is also necessary to ensure the speed of calculation. In this paper, the speed of the two algorithms is tested by MATLAB on the hardware platform of Intel Quad-Core i5-4590 with a 3.3 GHz CPU and 4 GB memory. The solution time of the least square coefficient fitting is 0.00063 seconds, and the solution time of the proposed algorithm is 0.019382 seconds. Although the solution time of the proposed algorithm is increased by 0.018752 seconds, it can all realize the solution work of the piezoelectric 6-dimensional accelerometer.

4. Conclusions

To enhance the measurement accuracy of 6-dimensional accelerometer, this work analyzes the cross coupling principle of piezoelectric 6-dimensional accelerometer and designs the linearity and non-linearity fitting method. The hybrid compensation algorithm based on two-stage calibration was proposed based on the cross coupling characteristics, and an experimental prototype of the piezoelectric 6-dimensional accelerometer was made. Ten groups of calibration experiments and ten groups of test experiments were carried out, as well as the calculation speed test of the algorithm. Compared with traditional algorithms, the effectiveness of the proposed algorithm is verified. The research conclusions are as follows:

- Based on the linear vibrostand and angular vibrostand with 6-dimensional acceleration load, install fixture method for linear calibration matrix and non-linear calibration matrix, by the method of sensor test experiment at the same time, can get the accelerometer measurements of 6 dimensions, that through the vibrostand with install fixture method can calibrate experiment and test.
- The proposed algorithm can measure the acceleration values in six directions when the single direction load is applied in the test experiment. The closer the non-linearity of the test results is to zero, the better the linearity of the measurement results and the higher the measurement accuracy. The average non-linearity of the six directions is 0.4559%, and the average non-linearity of the traditional method is 2.7186%. Compared with the traditional method, the average non-linearity of the proposed algorithm is 2.2628% lower.
- Compared with the traditional method, the non-linearity of the proposed algorithm decreases by 0.1124%-0.65% in the linear direction, and the non-linearity decreases by 3.8019%-4.2973% in the angular direction, indicating that the cross coupling of the piezoelectric 6-dimensional accelerometer mainly affects the accuracy of the angular direction. The proposed algorithm can effectively reduce the angular non-linearity and improve the accelerometer's overall measurement accuracy.
- The total ARE-2N value of the six directions of the proposed algorithm is 4.6309%, and the total ARE-2N value of the six directions of the least square method is 18.4291%. The total ARE-2N value of the six directions of the proposed algorithm decreases by 13.7982%, indicating that the proposed algorithm can effectively improve the measurement accuracy.
- The fitting solution time of the least square coefficient is 0.00063 seconds, the solution time of the proposed algorithm is 0.019382 seconds, and the solution time of the proposed algorithm is increased by 0.018752 seconds. Due to the feature fusion and online update of the algorithm processing, the processing steps are more than the traditional method, so that the solution time will be increased. However, all of them can realize the real-time solution of the piezoelectric 6-dimensional accelerometer.

Acknowledgments

This work was supported in part by the Fundamental Research Funds for the Natural Science Foundation Project of China. (Grant No. 52175494), and the National Key Research and Development Program of China. (Grant No. 2022YFB3206702).

References

Al-Mai, O., Ahmadi, M. and Albert, J. (2018), "Design, development and calibration of a lightweight, compliant six-axis optical force/torque sensor", *IEEE Sensor. J.*, **18**(17), 7005-7014. https://doi.org/10.1109/JSEN.2018.2856098.

Amini, A., Mohammadimehr, M. and Faraji, A. (2020), "Optimal placement of piezoelectric actuator/senor patches pair in sandwich plate by improved genetic algorithm", *Smart Struct. Syst.*, **26**(06), 721-733. https://doi.org/10.12989/sss.2020.26.6.721.

Chapsky, V., Portman, V.T. and Sandler, B.Z. (2007), "Single-mass 6-DOF isotropic accelerometer with segmented PSD sensors", *Sensor. Actuat. A-Phys.*, **135**(02), 558-569. https://doi.org/10.1016/j.sna.2006.10.024.

IOS 16063-21:2003 (E), Methods for the Calibration of Vibration and Shock Transducers-Vibration Calibration by Comparison to a Reference Transducer.

Li, J.Q., Zhang, Y.F., Chen, Z.Z., Wang, J., Fang, M., Luo, C.W. and Wang, H.H. (2020), "A novel edge-enabled SLAM solution using projected depth image information", *Neur. Comput. Appl.*, **32**(19), 15369-15381. https://doi.org/10.1007/s00521-019-04156-2.

Lin, S. and Sun, L. (2019), "Error analysis of the orthogonal parallel calibration device for six-axis heavy force sensor", *IOP Conf. Ser.: Earth Environ. Sci.*, **267**(4), 042167. https://doi.org/10.1088/1755-1315/267/4/042167.

Meng, Y., Wang, W., Han, H. and Ban, J.X. (2019), "A visual/inertial integrated landing guidance method for UAV landing on the ship", *Aerosp. Sci. Technol.*, **85**, 474-480. https://doi.org/10.1016/j.ast.2018.12.030.

Noureldin, A., Karamat, T.B., Eberts, M.D. and El-Shafie, A. (2009), "Performance enhancement of MEMS-based INS/GPS integration for low-cost navigation applications", *IEEE Trans. Vehic. Technol.*, **58**(03), 1077-1096. https://doi.org/10.1109/TVT.2008.926076.

Peng, Y.K. and Golnaraghi, M.F. (2004), "A vector-based gyro-free inertial navigation system by integrating existing accelerometer network in a passenger vehicle", *2004 Position Location and Navigation Symposium*, Monterey, CA, April.

Santoli, F., Fiorenza, E., Lefevre, C., Lucchesi, D.M., Lucente, M., Magnafico, C., Morbidini, A., Peron, R. and Iafolla, V. (2020), "ISA, a high sensitivity accelerometer in the interplanetary space updates after the near-earth commissioning phase of italian spring accelerometer-ISA", *Space Sci. Rev.*, **216**(08), 145. https://doi.org/10.1007/s11214-020-00768-6.

Sun, Y.J., Liu, Y.W. and Liu, H. (2016), "Temperature compensation for a six-axis force/torque sensor based on the particle swarm optimization least square support vector machine for space manipulator", *IEEE Sensor. J.*, **16**(03), 798-805. https://doi.org/10.1109/JSEN.2015.2485258.

Wang, D.H. and Yuan, G. (2011), "A six-degree-of-freedom acceleration sensing method based on six coplanar single-axis accelerometers", *IEEE Trans. Instrum. Measure.*, **60**(04), 1433-1442. https://doi.org/10.1109/TIM.2010.2083331.

Wang, X.H. (2008), "Non-linearity estimation and temperature compensation of capacitor pressure sensors using least square support vector regression", *International Symposium on Knowledge Acquisition and Modeling*, Wuhan, China.

Wang, Z.J., Yao, J.T., Hou, Y.L. and Zhao, Y.S. (2011), "Errors analysis and compensation of six-axis force sensor based on stewart platform", *Adv. Mater. Res.*, **317-319**, 1041-1044. https://doi.org/10.4028/www.scientific.net/AMR.317-319.1041.

Zhang, D.Z., Li M., Qin, L., Zhang Y.X., Liu, J.C. and Liu, J. (2021), "Analytical modeling of piezoelectric 6-degree-of-freedom accelerometer about cross-coupling degree", *Measure.*, **181**, 109630. https://doi.org/10.1016/j.measurement.2021.109630.

Zhao, Y.Z., Zhang, C.F., Zhang, D., Shi, Z.P. and Zhao, T.S. (2016), "Mathematical model and calibration experiment of a large measurement range flexible joints 6-UPUR six-axis force sensor", *Sensor.*, **16**(08), 1271. https://doi.org/10.3390/s16081271.

Zhou, Z., Shi, J., Yao, B.Y. and Feng, L.S. (2015), "Theoretical investigation of the mechanical coupling in a differential vibrating beam accelerometer", *Microsyst. Technol.*, **21**(07), 1459-1464. https://doi.org/10.1007/s00542-014-2224-6.